Exposure and Health (2021) 13:105–118
https://doi.org/10.1007/s12403-020-00366-5

ORIGINAL PAPER

Physicochemical Characterization of Personal Exposures to Smoke Aerosol and PAHs of Wildland Firefighters in Prescribed Fires

Jordan Nelson[1] · Marie-Cecile G. Chalbot[1,2] · Irini Tsiodra[3] · Nikolaos Mihalopoulos[3] · Ilias G. Kavouras[1,4]

Received: 25 February 2020 / Revised: 25 May 2020 / Accepted: 5 June 2020 / Published online: 11 June 2020

Abstract

Particle mass and number of smoke aerosol exposures of firefighters were studied during prescribed fire events. In addition, organic and elemental carbon, functional content and polynuclear aromatic hydrocarbons were determined by spectrometric and chromatographic methods. During the study, firefighters engaged in working tasks including maintenance of the fire front using drip torch ignition and support activities related to fire progression monitoring. Particle number concentration was dominated by particles in the fine range (diameter 0.5–2.5 µm) including significant quantities (about 10–30%) of coarse particles (diameter > 2.5 µm). Particle number concentrations varied substantially during a fire event and were related to topography as well as firefighter's activity with elevated particle number concentrations during increased walking speeds. This variation was in agreement with the median and standard deviation of the percent relative concentration difference values indicating within-subject variability. Both organic and elemental carbon were accumulated in particles with a diameter lower than 1.0 µm. Combustion 4- and 5-ring PAHs including pyrene, chrysene and benzo[a]pyrene were accumulated in fine aerosol, with naphthalene being present mostly in larger particles. The values of PAHs concentration diagnostic ratios indicated a mixture of biomass burning and fossil fuel combustion probably due to the use of gasoline and diesel to ignite the fire. These findings may also be relevant for environmental exposures to wildfires smoke because of the proximity of large and intense wildfires in populated centers.

Keywords NMR spectroscopy · GC/MS · Functional composition · Benzo(a)pyrene · Wildfire smoke · Particle number

Introduction

Firefighters comprise the largest group of public safety employees with more than 373,600 career and 682,600 volunteer firefighters in the United States (US) responding to different fire types including structural and wildfires (Haynes and Stein, 2017; Evarts and Stein, 2019). As a result, firefighters are routinely exposed to chemical, physical, and psychological stressors with smoke inhalation being the predominant risk factor associated with disease onset (Adetona et al. 2013a; Banes 2014). Wildfires smoke has been associated with increased risk of respiratory and cardiovascular diseases including COPD, acute bronchitis, pneumonia (Delfino et al. 2008; Morgan et al. 2010), cardiovascular mortality (Soteriadis et al. 2011, Rappold et al. 2011) and cancer (Daniels et al. 2014, 2015) among firefighters and the general public. However, the specific component(s) of smoke responsible for the onset of health outcomes has yet to be elucidated. Respiratory protection is afforded to firefighters responding to structural fires, but their use in wildland firefighting is limited due to device weight and fixed air capacity (Austin et al. 2001; Fabian et al. 2011). Towels and bandanas over firefighter's mouth and distance from the fire are the most frequent methods to prevent smoke inhalation during an active wildfire event.

✉ Ilias G. Kavouras
ilias.kavouras@sph.cuny.edu

1 Department of Environmental Health Sciences, Ryals School of Public Health, University of Alabamaa Birmingham, Birmingham 35219, USA

2 Department of Biology, College of Technology, City University of New York, Brooklyn 12222, USA

3 Environmental Chemical Processes Laboratory, Department of Chemistry, University of Crete, 70013 Heraklion, Greece

4 Department of Environmental, Occupational and Geospatial Health Sciences, Graduate School of Public Health and Health Policy, City University of New York, New York 10027, USA

Deteriorated lung function, oxidative damage, and inflammatory responses have been observed in firefighters; albeit only a handful of these studies simultaneously collected exposure measurements (Greven et al. 2011; Adetona et al. 2013b; Hejl et al. 2013; Gaughan et al. 2014). The inherit dangers, unpredictable nature, variable duration, and remote location of wildfires makes it uniquely challenging for exposure monitoring. In particular, monitoring of exposures during wildfires is limited due to equipment interfering with the firefighters' physically demanding activities; resulting in safety concerns for both firefighters and research personnel. Adding to safety and logistical challenges, smoke is a variant, complex, and heterogeneous mixture of predominantly carbonaceous (elemental and organic carbon) aerosols. While many organic compounds have been identified, they have only been reported as accounting for up to 20% of the particulate mass due to limitations associated with extraction, fractionation, and derivatization steps in chromatographic analysis (Kavouras and Stephanou, 2002a, b; Pöschl, 2005). Previous studies have utilized spectroscopy to determine the functional content and molecular profile of smoke aerosol (Decesari et al. 2006; Chalbot et al. 2013). Chalbot et al. (2016) determined a strong aromatic signature for fresh biomass burning aerosol that transitioned to oxidized carbonyl and carboxyl organic species in aged smoke. Differences in the chemical content of smoke may have the ability to modify the biological and toxicological responses to smoke aerosol. However, there are still many knowledge gaps in wildland biomass smoke chemical content that need to be addressed in order to understand and prevent onset and/or progression of associated diseases in firefighters who may be adversely exposed to fresh wildfire smoke aerosol.

Prescribed fires (R_x) are managed fires used in forest management, restoration of native vegetation, and farming to reduce the accumulation of dry biomass fuel and lessen the likelihood of fast-spreading and destructive wildfires. In the contiguous US, there were 450,335 R_x fires that consumed over 6 million acres and 58,083 wildfires that consumed approximately 8.8 million acres during the year 2018 (NFIC, 2018). In R_x fires, firefighters and management personnel ignite a fire line and work within the smoke plume to actively manage the fire's front, progression, and boundaries. To manage the progression of a R_x fire, backing and/or flanking methods are used. In these conditions, fire progression moves against the wind (downslope) producing lower flame heights, lower fire intensity, and moves through the stand of vegetation at slower speed than head fires. Flanking fires are set perpendicular to backfires aiming to speed the backfire process. As a result, firefighters are typically within or in close proximity of the smoke plume throughout the entire work-shift. During R_x fire, firefighters are reported as being exposed to comparable (or higher) levels of respirable particulate mass, carbon monoxide, acrolein, formaldehyde, and benzene in comparison to exposures during wildfires (Reinhardt and Ottmar 2004; Gaughan et al. 2014; Miranda et al. 2010). Additionally, collection of exposure measures during R_x fire affords the unique opportunity to obtain precise and realistic field occupational exposure from active duty firefighters immediately before, during, and immediately after involvement in active fires.

The objective of this study was to characterize the chemical fingerprint and spatiotemporal variation of personal exposures of firefighters to smoke aerosol in R_x fires. This was achieved by *in-situ* monitoring of personal exposures using continuous and integrated aerosol devices during active R_x fire events. The use of R_x fires was essential in achieving the objectives of the study since it facilitates measurement obtainment during typical field conditions without interfering with the duties and the safety of the firefighter's or research personnel. We characterized the biologically relevant water-soluble fraction of smoke exposures by nuclear magnetic resonance (NMR) spectroscopy in its entirety without fractionation or derivatization (Chalbot and Kavouras 2014), the size distribution of polynuclear aromatic hydrocarbons (PAHs) (Kavouras et al. 1998) and geospatially-enabled fine and coarse particle number concentrations.

Materials and Methods

R_x Fire Sites

Personal exposures to firefighters were monitored in sixteen backing or flanking R_x fires performed by The Nature Conservancy's crews in central Alabama (Fig. 1). The predominant objective of the R_x fires was to control invasive species encroachment and promote the growth of native vegetation. Measurements were obtained from 29 unique individuals resulting in 81 individual personal exposure measurements with repeats (i.e. measurements on the same subjects) ranging from 1 to 13.

Table 1 shows the characteristics of the R_x fires, number and type of personal exposure measurements. R_x plots #1, 3–8, 11 and 13 were located adjacent to Cahaba River National Wildlife Refuge in central Alabama (33°2′32″ N 87°4′35″ W) (Fig. 1). Mountain longleaf pine (*Pinus palustris)* mixed with Virginia (*Pinus virginiana*), shortleaf (*Pinus echinata*) and loblolly (*Pinus taeda*) pine were the dominant tree species. Longleaf pine forests depend on fires to facilitate growth and can evolve into hardwood communities without fire. The ground cover included low-growing blueberries, huckleberries, various bluestems, Indian grass and other herbaceous plants. R_x plots #2, 9, 14 and 16 were located in the Camp Tukabatchee (N32° 40′ 23.7′ N, 86° 36″ 51.66″ W) on Warner Scout Reservation (Fig. 1). Finally, the

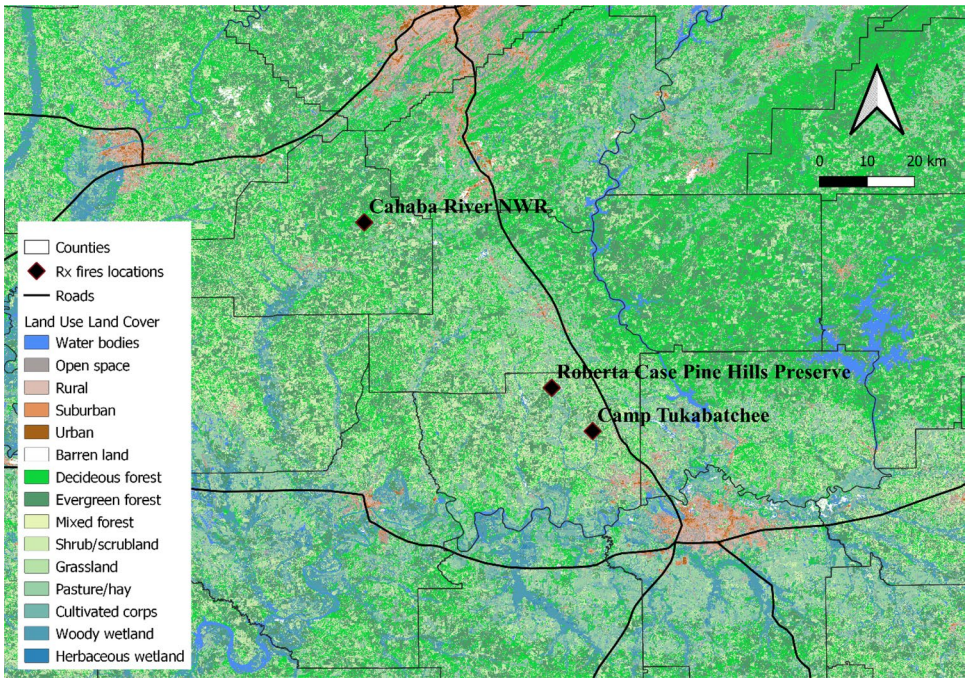

Fig. 1 The three locations of the R_x fire plots in central Alabama and land use/land cover (2016 National Land Cover Database)

Table 1 Characteristics of R_x fires (biomass type, burnt area and duration of the event), number of participants and personal exposure measurements in each R_x fire

R_x	Biomass type description	Burnt area (km^2)	Duration (h)	Fire crew	Personal exposure measurement
1	Longleaf/loblolly pine; pine needles, hardwoods; underbrush/litter	0.40	6.5	6	Integrated QFF filter for EC/OC and NMR analysis
2		0.24	4.0	6	
3		0.22	3.5	6	
4		0.55	8.0	6	Continuous particle number concentration
5		1.60	6.0	10	
6		0.46	7.0	5	
7		0.65	8.0	6	
8		0.24	6.5	6	
9	Mixed pasture/grass and longleaf pine; head fire	0.64	5.0	4	
10	Longleaf/loblolly pine; pine needles, hardwoods; underbrush/litter	0.36	5.5	6	
11		0.56	6.5	6	
12	Grass	0.48	6.2	6	
13	Long leaf pine plantation	2.66	5.0	8	Continuous particle number concentration + Cascade impactor (PAHs analysis)
14	Longleaf/loblolly pine; pine needles, hardwoods; underbrush/litter	0.30	5.0	4	
15	Grass	0.52	6.8	6	
16	Longleaf/loblolly pine; pine needles, hardwoods; underbrush/litter; sand acer plane; some old structures within burn unit	0.46	6.0	8	

#10, 12 and 15 R_x plots were at the Pine Hills Hunting Area within the Roberta Case Pine Hills Preserve (32°29′56.7″N, 86°29′28.6″W) (Fig. 1). The preserve is approximately 400 acres of mixed longleaf pine forest with a couple open pasture and grassland fields. It hosts the Alabama Canebrake pitcher plant (*Sarracenia rubra* ssp. *alabamensis*) and Harper's ginger plant (*Hexastylis speciosa*). These properties are maintained with R_x fires by TNC every 2–3 years.

The R_x fires were ignited with a heavy drip-torch and re-ignited as necessary to promote advancement of the fire

front. Mixed conditions (flaming and smoldering) were abundant during the R_x fires. However, ignition and flaming phases dominated the early stages of the fires, whereas, smoldering characteristics were observed during the later stages of the fire. The burnt area ranged from 0.22 to 2.66 km^2 for a total of 9.48 km^2 (mean of 0.65 km^2/ R_x) (Table 1). The R_x fires were typically initiated in the morning (9:00–10:00 am) and lasted an average of 6.0 h (from 3.5 to 8 h). An average crew of 6 firefighters burnt approximately $70–80 \times 10^3$ m^2 per hour. Additional crew members were deployed for larger R_x fires.

Exposure Monitoring

The characterization of smoke exposure was done as follows: (i) collection of personal total suspended particles (TSP) on a filter and subsequent chemical analysis by ^{1}H-NMR spectroscopy and thermal/optical reflectance (TOR) analysis (18 samples in three R_x fires); (ii) continuous monitoring of fine (with diameter between 0.5 and 2.5 µm) and coarse (with diameter greater than 2.5 µm) particle number concentrations (81 samples in 13 R_x fires) and (ii) collection of size fractionated aerosol samples and analysis for PAHs and TOR analysis (4 samples in 4 R_x fires). Concurrent personal continuous and integrated monitoring was only possible for a subset of measurements due to safety concerns and backpack weight limitation carried by firefighters.

WSOC and Functional Analysis by ^{1}H-NMR Spectroscopy

For TSP sampling, personal exposure samples were collected on quartz fiber filters (QFF) using a SureSeal™ filter cassettes attached to small battery-powered pump (AirCheck XR5000, SKC Inc., Eighty Four, PA). QFFs were purchased from Whatman (QM-A grade, Tisch Environmental Inc, Cleves, OH). These filters were pre-combusted at 550 °C for 4 h and then kept in a dedicated clean glass container with silica gel to avoid humidity and contamination. The sampler was turned on when the participants left at the staging area (approximately 5–10 min prior to the initiation of R_x fire) and turned off upon their return to the staging area, between 5–15 min after the completion of the R_x fire. TSP mass measurements were obtained using a microbalance (Mettler-Toledo LLC, Columbus, OH). The detection limit and relative standard deviation for mass measurements were 10 µg m^{-3} and 5%, respectively. A 1-cm piece of the filter was analyzed for organic (four fractions evolved at 140 °C (OC1, volatile), 280 °C (OC2, semivolatile), 480 °C (OC3, nonvolatile) and 580 °C (OC4, nonvolatile) and pyrolyzed OC (POC) in a He-only atmosphere) and elemental (three fractions evolved at 580 °C (EC1, volatile), 740 °C (EC2, semivolatile) and 840 °C (EC3, nonvolatile) in a 98% He/2%O_2 atmosphere) carbon by TOR (DRI Model 1000 analyzer (Atmoslytic Inc., Calabasas, CA); Chow et al. 2001). POC is defined as the carbon evolved at 580 °C by the addition of 2% O_2.

The remaining filter was extracted by sonication with 5 mL of ultrapure H_2O for 1 h. The water-soluble extract was dried under vacuum and reconstituted in 700 µL of a TSP-d_4 (2,2,3,3-d_4-3-(trimethylsilyl)propionic acid sodium salt, 0.248 µmol mL^{-1}, Internal Standard), 0.2 M Na_2HPO_4/0.2 M NaH_2PO_4 (disodium phosphate/monosodium phosphate, pH 7.4) and sodium azide (NaN_3; 1% w/w) in D_2O solution. ^{1}H-NMR spectra were acquired using a Bruker Advance III spectrometer operating at 600.17 MHz ($B_0 = 18.8$ T) as described previously (Chalbot et al. 2014, 2016). The NMR spectra were integrated in five spectral regions representing different non-exchangeable hydrogen types as follows: (i) δ_H 0.6–1.8 ppm: alkyl (H–C), included R–CH_3, R–CH_2, and R–CH hydrogen atoms; (ii) δ_H 1.8–3.2 ppm: alllylic (H–C–C=); (iii) δ_H 3.2–4.4 ppm: saturated oxygenated (H–C–O), containing hydrogen atoms adjacent to alcohols, ethers and ester functionalities; (iv) δ_H 5.0–6.4 ppm: acetalic/vinylic (O–CH–O and H–C=), included hydrogen atoms of olefins, ethers, esters and organic nitrates; and (v) δ_H 6.5–8.3 ppm: aryl (H–Ar).

Continuous Particle Monitoring

Continuous particle number concentrations (PNC) were measured using the Dylos1700 (Dylos Corp., Riverside, CA) particle counter by light-scattering to count particles in two size ranges, particles with diameter greater than 0.5 ($PNC_{>0.5}$) and 2.5 µm ($PNC_{>2.5}$). Fine PNC was calculated as the difference between the two counts ($PNC_{0.5–2.5} = PNC_{>0.5} – PNC_{>2.5}$). The Dylos particle counter has been previously used in indoor, outdoor, personal environmental, and occupational studies (Northcross et al. 2013; Brown et al. 2014; Steile et al. 2015; Sousan et al. 2016). The monitor was attached on the backpack of the firefighters with elastic cord attachments to secure it. Protective plastic covers were placed over the control board and a coarse screen was installed on the inlet to prevent the entrainment of larger objects that may interfere with the sensor and the fan. The monitors were compared to particle size distribution and mass concentrations measured by MSP 1000XP Wide Particle Spectrometer using laboratory generated aerosol ($R^2 > 0.90$). In addition, the location (latitude and longitude), altitude, speed, and distance traveled in 1-min intervals of each participant was continuously recorded using a Garmin eTrex10 GPS device equipped with HotFix satellite prediction technology to maintain satellite reception under dense vegetative cover. 1-min averages were stored on the instrument. We calculated R_x fire averages if at least 66% of the time period had valid data. To eliminate erroneous

data, measurements were excluded if measured $PNC_{>0.5}$ or $PNC_{>2.5}$ or computed $PNC_{0.5–2.5}$ were negative. This resulted in less than 0.5% deletions of the original. The majority of these deletions were due to very low counts at the beginning of the monitoring or after extremely high counts probably due to the saturation of the sensor.

OC, EC and PAHs Size Distribution

A Model 298 Marple personal cascade impactor mounted to a battery-powered pump (AirCheck XR5000, SKC Inc., Eighty Four, PA) was used to collect smoke aerosol samples into eight particle size fractions on quartz fiber filters, according to their aerodynamic cutoff diameters at 50% efficiency: (i) the first stage: > 21.3 μm; (ii) second stage: 21.3–14.8 μm; (iii) third stage: 14.8–9.8 μm; (iv) fourth stage: 9.8–6.0 μm; (v) fifth stage: 6.0–3.5 μm; (vi) sixth stage: 3.5–1.55 μm, (vii) seventh stage: 1.55–0.93 μm; and (viii) eighth stage: 0.93–0.52 μm at a nominal flow rate of 2 L min^{-1}. An upper limit of 30 μm for the larger particles was assumed based on the effective cut-point of the inlet. After collection, filters were folded and wrapped in aluminum foil and stored in a freezer at − 30 °C until extraction and analysis. A set of filters were analyzed for OC and EC as described previously (Sect. 2.2.1). The second set of filters was analyzed for PAHs as previously described (Gogou et al. 1998). The recovery of PAHs varied from 72% for naphthalene to 99% for chrysene and benzofluoranthenes. PAHs concentration diagnostic ratios were used to reconcile their presence in the atmosphere (Kavouras et al. 2001, 2012) as follows: (i) Fluoranthene to (Fluoranthene + Pyrene): Fl/(Fl + Py); (ii) Benzo[a]anthracene to (Benzo[a]anthracene + Chrysene/Triphenylene): BaA/(BaA + CT); (iii) Benzo[e]pyrene to (Benzo[e]pyrene + Benzo[a]pyrene): BeP/(BeP + BaP)l and (iv) Indeno[1,2,3-cd]pyrene to (Indeno[1,2,3-cd]pyrene + Benzo[ghi]perylene): IP/(IP + BgP).

Statistical Analysis

Two-way analysis of variance (ANOVA) for TSP, EC, OC and functional composition and Kruskal–Wallis H-test for PNC (log-normal distribution) was applied to compare the measurements across multiple R_x fires and among participants within a single R_x fire (IBM SPSS, version 22.0, Chicago, IL). Note that to determine whether significant differences exist among firefighters and R_x fires with log-normal distribution, the geometric mean (μ) and standard deviation (σ) were used. To assess the variability of exposures among the participants the percent relative particle number concentration difference ($\%\Delta C/C_{fm}$) between the participant and the crew leader was computed (Lianou et al. 2007). The median percent relative difference is a metric of systematic differences between participants across all R_x fires (i.e. whether firefighters were exposed consistently higher (or lower) than the crew leader, whereas participant-to-participant variation is evaluated by the standard deviation of the percent relative difference. The crew leader was chosen as the reference measurement for consistency across all R_x fires. In addition to fire management tasks, the crew leader was also carrying out tasks related to oversight of R_x fire boundaries that could modify the exposure profile as compared to other crewmembers. The locations and particle number concentrations were geospatially analyzed to calculate the gridded (100 m × 100 m) average exposures in each R_x fire plot (QGIS3.4.16).

Results and Discussion

TSP, EC, OC and Functional Non-exchangeable Hydrogen Composition

The mean ± 3 s (minimum and maximum in parentheses) levels of TSP mass, OC, EC, non-exchangeable organic alkyl, allylic, oxygenated, acetalic + vinylic and aryl hydrogen concentrations, specific molecular markers in personal exposures are presented in Table 2. TSP personal exposures varied from 0.7 mg m^{-3} to 5.6 mg/m^3 with mean TSP mass concentration of 2.3 ± 0.2 mg m^{-3}. OC levels ranged from 153 μgC m^{-3} to 2,018 μgC m^{-3} with average concentrations of 586 ± 112 μgC m^{-3}. EC levels varied from 33 μgC m^{-3} to 343 μgC m^{-3} with average of 130 ± 20 μgC m^{-3}. They were comparable to those previously measured in R_x fires and hot-spot wildland firefighters (Reinhardt and Ottmar 2004; Miranda et al. 2010). The OC/EC ratio (5.1 ± 0.7) was indicative of mixed vegetation combustion; from 1.45 in early/ignition phases up to 11.69 in subsequent phases (Kavouras et al. 2012). In this study, ignition and fire management occurred throughout the R_x fire, as the fire front was continuously maintained through re-ignition. Assuming a conversion factor of organic carbon to organic mass (OC-to-OM) equal to 3.1, the reconstructed OC and EC accounted for up to 98% of measured TSP mass (Kavouras et al. 2012). This was comparable to the overall contribution of carbonaceous aerosol to particle mass in R_x fires and was attributed to the potential for the release of soil organic matter particles by rapidly changing wind patterns and turbulence ahead of the fire front. It was further corroborated by the relative distribution of OC fractions with maximum for OC3 (compounds evolved at temperatures between 280 and 480 °C) (Fig. 2). OC3 was the predominant OC fraction in sites heavily impacted by biomass burning (Pani et al. 2019). Although we did not measure soil minerals (i.e. Si, Al, Fe and Ca) in this study; soil elements accounted for no more than 2.5% of particle mass in R_x fires (Kavouras et al. 2012).

Table 2 Personal exposure concentrations of TSP, OC, EC, non-exchangeable hydrogen types and molecular markers concentrations [mean (±3 s) and min–max (in parentheses)], 1-min fine (0.5–2.5 µm) and coarse (>2.5 µm) PNC [median (μ) and min–max (in parentheses)] of firefighters in R_x events, and the median (μ) and σ of the relative concentration difference

Variable	Concentration	$\%\Delta C/C_{ref}$	
		μ	σ
Particulate matter [R_x fires: 1, 2 and 3]			
TSP mass (mg m^{-3})	2.3 ± 0.2 (0.7–5.6)	− 34.6	50.7
OC (µg m^{-3})	586 ± 112 (153–2,018)	4.3	90.3
EC (µg m^{-3})	130 ± 20 (33–343)	62.5	93.2
OC/EC conc. ratio	5.1 ± 0.7		
Non-exchangeable hydrogen (µmolH m^{-3}) [R_x fires: 1, 2 and 3]			
Alkyl (H–C)	7.1 ± 2.1 (2.0–42.5)	16.3	45.0
Allylic (H–C–C=)	4.3 ± 1.1 (1.1–21.3)	7.1	68.5
Oxygenated (H–C–O)	7.2 ± 1.6 (1.1–29.0)	− 23.1	77.6
Acetalic (O–CH–O) and vinylic (H–C=)	0.7 ± 0.1 (0.1–2.6)	− 18.0	86.3
Aryl (H–Ar)	1.0 ± 0.2 (0.2–3.0)	− 17.3	99.9
Molar H/C ratio	0.42 ± 0.05		
Molecular markers (µg m^{-3}) [R_x fires: 1, 2 and 3]			
Levoglucosan	0.90 ± 0.20 (0.05–3.47)	− 8.0	224.1
Formate	0.16 ± 0.05 (0.02–0.76)	24.4	92.6
Acetate	0.29 ± 0.05 (0.11–0.87)	32.5	35.0
Succinate	0.60 ± 0.10 (0.22–1.95)	19.1	62.6
Lactate	1.80 ± 0.20 (0.71–3.64)	19.3	86.9
Particle number concentration (part L^{-1}) [R_x fires: 4–16]			
Fine PNC	19,545 (3–216,876)	− 14.1	219.9
Coarse PNC	1,411 (3–190,419)	− 13.0	482.1

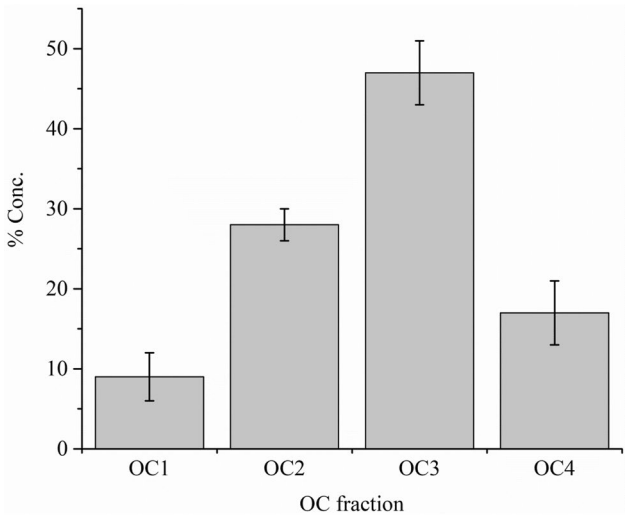

Fig. 2 The relative concentration distribution of OC fractions in personal exposures

Table 2 also shows the median (µ) and σ of the $\%\Delta C/C_{ref}$ of TSP mass, OC, EC, non-exchangeable organic alkyl, allylic, oxygenated, acetalic + vinylic and aryl hydrogen concentrations and specific molecular markers. Negative $\%\Delta C/C_{ref}$ values indicated that crew leader concentrations were higher than those measured for other crewmembers at the same time. The median $\%\Delta C/C_{ref}$ for TSP (ca. − 34.6%) may be associated with a potentially increased contribution of coarse soil particles generated by an all-terrain vehicle used by the crew leaders to monitor the fire boundaries. The highest median $\%\Delta C/C_{ref}$ was computed for EC (62.5%), which may be indicative of sporadic exposures to primary EC during smoldering or ignition at close proximity to the firefighter. The majority of the R_x fires in this study were backing fires where firefighters were continuously following the fire front through smoldering conditions, reigniting the fire line as needed. Low to moderate $\%\Delta C/C_{ref}$ for OC, non-exchangeable organic hydrogen and organic species indicated little difference in exposure between the crew leaders and members. However, high $\%\Delta C/C_{ref}$ σ values indicated strong firefighter-to-firefighter variations probably due to different activity patterns and localized fire conditions. Crewmembers have different tasks ranging from actively maintaining the fire using a drip torch, monitoring the fire boundaries and supporting fire progression. As a result, exposures to chemical species emitted during combustion could vary substantially.

Figure 3a–c show a representative ^{1}H-NMR spectra of the personal exposures water-soluble extract, the structures of five molecular markers and the functional distribution plot of personal exposures, respectively. Both sharp resonances associated with the *abundant organic species and an envelope of* convoluted resonances, shown by the baseline hump in the aliphatic saturated and unsaturated range consistent with the presence of soil humic and fulvic acids, were observed (Chalbot et al. 2013). Non-exchangeable saturated oxygenated (H–C–O) (7.2 ± 1.6 (1.1–29.0) µmolH m^{-3}) and alkyl (H–C) (7.1 ± 2.1 (2.0–42.5) µmolH m^{-3}) were the predominant types of hydrogen accounting for 38% and 32% of total non-exchangeable organic hydrogen, respectively. This was followed by aliphatic allylic (H–C–C=) (4.3 ± 1.1 (1.1–21.3) µmolH m^{-3}; 21%) and aryl (H–Ar) (1.0 ± 0.2 (0.2–3.0) µmolH m^{-3}; 6%) non-exchangeable organic hydrogen (Table 2). The functional distribution was comparable to the relative distribution of non-exchangeable hydrogen types in fresh wood burning indicating the release of oxygenated compounds (Chalbot et al. 2014; Chalbot and Kavouras 2019). Differences in the relative abundance of saturated alkyl and allylic in wood burning and personal exposures may be attributed to higher emissions of unsaturated species during smoldering of wood combustion in fireplaces as compared to charring in R_x fires. The mean H/C molar ratio (0.42 ± 0.05) was comparable to those previously measured

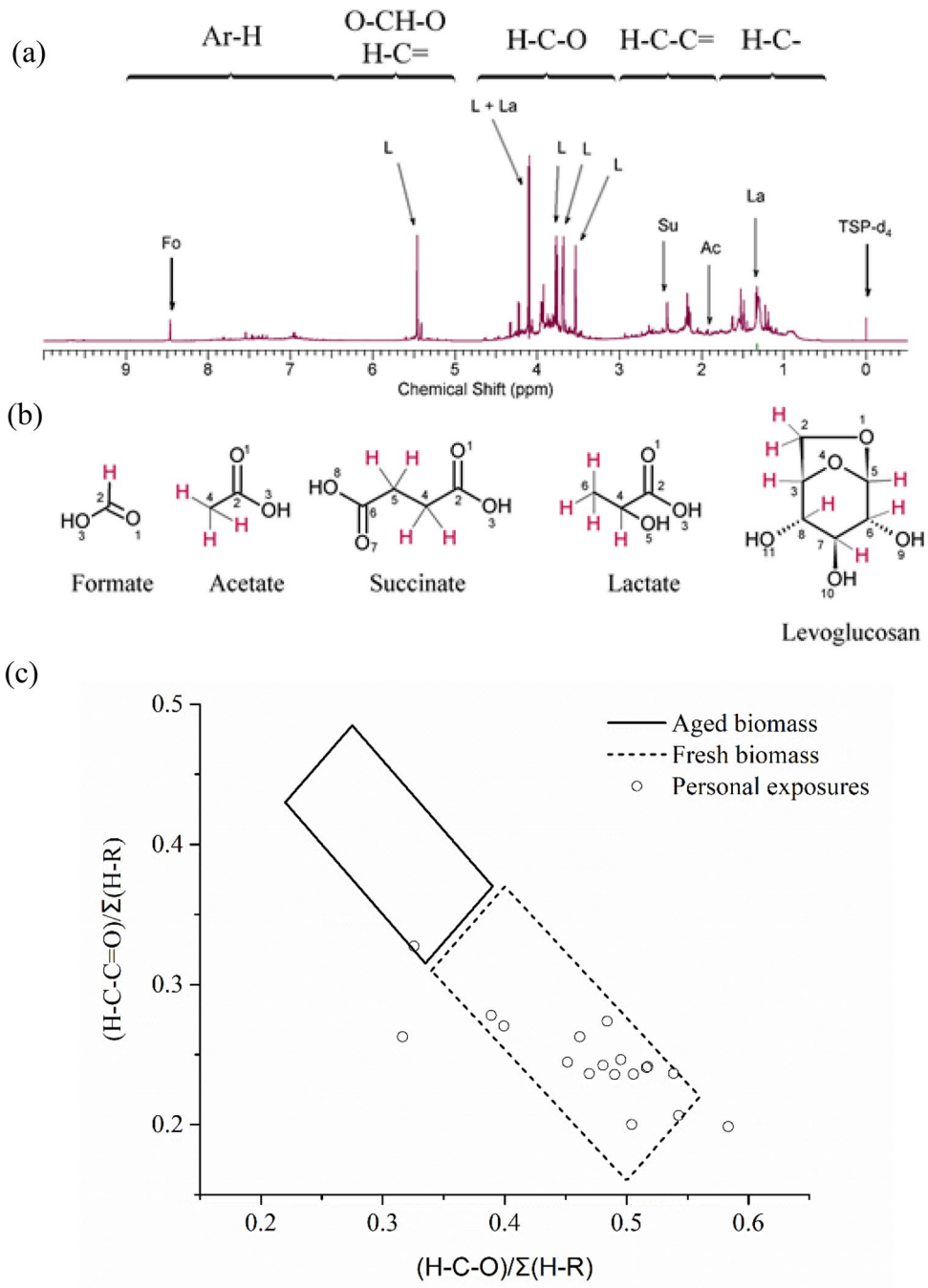

Fig. 3 **a** Representative 600 MHz ^{1}H-NMR spectrum, **b** structures of identified chemical compounds and **c** functional group distribution of personal exposures to smoke. (*L* levoglucosan, *Fo* formate, *Su* succinate, *Ac* acetate, *La* lactateTSP-d_4:3-(trimethylsilyl) propionic-2,23,3-d_4 acid sodium salt) (H–C–: alkyl hydrogen, H–C–C=: allylic hydrogen, H–C–O: oxygenated hydrogen, O–CH–O: acetalic hydrogen, H–C=: vinylic hydrogen, Ar–H: aromatic hydrogen)

for vegetation combustion (0.39) and downwind of R_x fires (0.64–0.68), suggesting a strong polyaromatic content that is typically observed in combustion-related process (Adler et al. 2011; Chalbot et al. 2013). However, the molar H/C ratio should be cautiously evaluated because of the inherent inability of NMR spectroscopy of aqueous samples to identify liable protons in hydroxyl, carboxylic and amine functional groups due to H/D exchange (Duarte et al. 2007).

Five organic compounds were identified by means of their NMR reference spectra. These were lactate (La in Fig. 3a, b; H-6, duplet at δ 1.33 ppm; H-4, multiplet at δ 4.12 ppm), acetate (Ac in Fig. 3a-b; H-4 at δ 1.92 ppm), succinate (Su in Fig. 3a, b; H-4 and H-5 at δ 2.41 ppm), levoglucosan (L in Fig. 3a, b; H-6, multiplet at δ 3.52 ppm; H-7 and H8, multiplet at δ 3.67; H2, multiplet at δ 3.73–3.75 ppm and at 4.08 ppm; H-5, singlet at 5.45 ppm; H-3 at 4.64 ppm was not visible of solvent residues) and formate (F in Fig. 3a, b; H-2, singlet at 8.47 ppm). Levoglucosan is a unique tracer of biomass burning emissions (Simoneit et al. 2004). These findings are consistent with those reported previously by the analysis water-soluble organic fraction of aerosol samples collected during the flaming phase of R_x

fires (Chalbot et al. 2013). Carboxylic acids (i.e. formate, acetate and succinate) may be associated with both biomass combustion and soil organic matter. Lactate had the highest concentrations (1.8 ± 0.2 µg m^{-3}), followed by levoglucosan (0.9 ± 0.2 µg m^{-3}) and succinate (0.6 ± 0.1 µg m^{-3}) (Table 2).

The ratios of α-carboxyl/keto (H–C–C=O) and oxygenated (H–C–O) to total aliphatic carbon (H–R) were calculated using molar H/C ratios of 2, 1.1, and 0.4 for non-exchangeable aliphatic alkyl and allylic, oxygenated and aryl hydrogen, respectively (Fuzzi et al. 2001). The α-carboxyl/keto carbon fraction was calculated by subtraction of the aromatic from aliphatic allylic carbon. The sum(H–R) carbon included saturated and unsaturated carbon in acids and ketones, aryl (H–Ar) and alkyl (H–C) hydrogen). The (H–C–C=O)/sum (H-R) ratio values ranged from 0.198 to 0.325 and (H–C–O)/sum(H–C) ratio values from 0.316 to 0.583 (Fig. 3c). These values were comparable to those calculated for fresh biomass burning emissions and were characteristic of the presence of polyols and anhydrides associated with fresh smoke particles (Chalbot et al. 2013, 2016).

Spatiotemporal Variability of Particle Number Exposures

The 1-min PNC varied from 3 to 216,876 part L^{-1} for the fine fraction and to 190,419 part L^{-1} for the coarse fraction, with a mean of 19,455 and 1296 part L^{-1}, respectively (Table 2). Personal PNC exposure of firefighters were higher than those measured at the staging area (median fine PNC: 5942 part L^{-1}, coarse PNC: 327 part L^{-1}; $p < 0.001$). Note that the staging area was impacted by smoke for most of the R_x fires, however, at considerably lower concentrations and for shorter durations (i.e. when the fire line was burning near the staging area or the wind redirected smoke outside of the burn unit). The fine PNC accounted for more than 70% of total (fine + coarse) particle number indicating that significant quantities of coarse particles may be released during fires. Similarly, coarse PM has been reported after large US wildfires to be a smaller, yet significant, contribution of wildfire smoke composition (Schweizer et al. 2019). Additionally, when compared to background levels, mean $PM_{2.5}$ concentrations had a greater increase in concentration between wildfire versus non-wildfire days in comparison to $PM_{2.5–10,}$ indicating a greater contribution of $PM_{2.5}$ from wildfire smoke than soil sources. This also supports the increased abundance of coarse particles being associated with soil organic matter, as indicated by OC and markers in smoke aerosol (Fig. 3 and Table 2).

The µ and 1σ range ($\mu - \mu/\sigma$ to $\mu + \mu \cdot \sigma$) of fine and coarse PNC levels for R_x fires #4–16 as well as the average distance travelled and change in elevation by firefighters for R_x fires #9–16 are depicted in Fig. 4. Differences of both fine and coarse PNC levels among firefighters were statistically significant ($p < 0.001$). This was consistent with the high $\%\Delta C/C_{ref}$ σ values (219.9 and 482.1; Table 2) indicating a strong variability among firefighters. However, for both fine and coarse PNC values, exposure conditions were comparable to those measured to the crew leader/fire manager for this study (as determined by the median $\%\Delta C/C_{ref}$ values). These fine PNC do not include particles with diameter less than 0.5 µm that typically account for the majority of PNC and thus may not comprehensively represent the fine fraction of particles available in biomass smoke. This is consistent with previous studies which showed variability in exposure based on the firefighting task. According to Adetona et al.

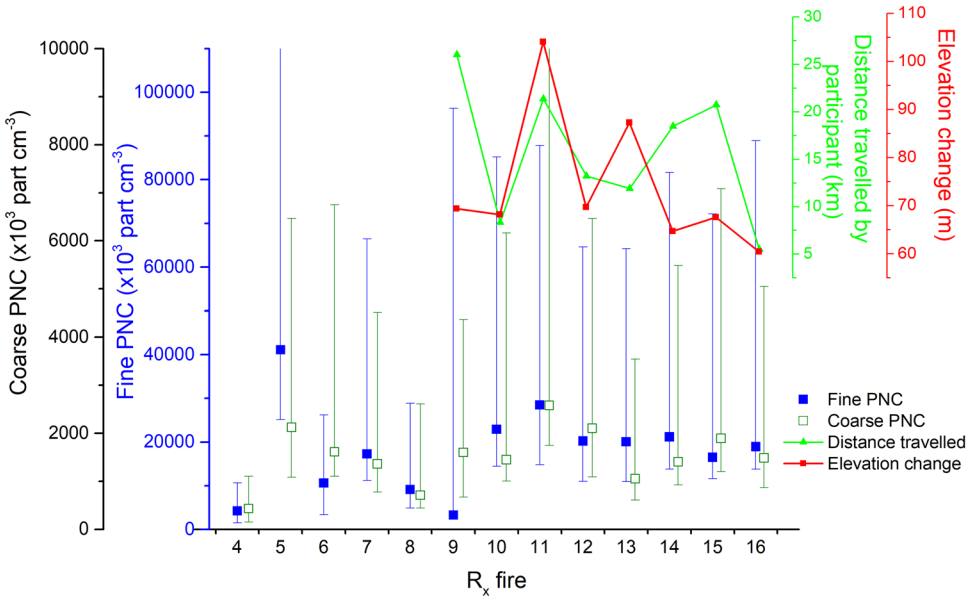

Fig. 4 Distribution of personal fine and coarse PNC for R_x fires 4–16, average distance travelled per participant and difference in elevation. The square is the median (μ) and the error bars are the range ($(\mu + \mu/\sigma, \mu + \mu \cdot \sigma)$)

(2013a), exposure intensity changed for firefighting of different working tasks where fire line holding and mop-up had the highest $PM_{2.5}$ exposures. There was no additional relationships evident between personal PNC levels and biomass type (woodland or grass), burnt area nor duration of the R_x fire. Therefore, these differences in particle concentration may be the result of firefighter location in relation to the fire front coupled with the intensity of the fire at that time point and weather conditions such as wind direction, wind speed, and humidity.

An example of the spatial variability of PNC is shown in Fig. 5a and b. The mean gridded (100 × 100 m) fine PNC portrayed highly variable exposure conditions during the fire with higher levels being measured in topographically favorable locations (i.e. on the base of the ridge). The firefighters monitored both the perimeter of the fire plot as well as walked within the plot to maintain the fire front. The fine PNC, walking speed (m s^{-1}) and elevation (meters above sea level, masl) were mapped for a firefighter in the R_x #12 fire revealing that approximately 50 min elapsed between the start of PNC monitoring at the staging area and exposure to elevated fine PNC (Fig. 5b). In that period, the firefighter joined the briefing by the fire manager and descended about 50 m to the base of the hill. During the fire, there were intermittent periods of moderate (between 1200 and 10,000 part L^{-1}) and high (higher than 10,000 part L^{-1}) PNC levels, indicating highly variable exposure patterns during the fire. The quartiles of PNC area measurements at the staging area were set as the threshold for moderate and high PNC exposure levels. High PNC levels were associated with increased walking speed as the firefighter was ascending or descending the hill to manage the wildfire. Low or moderate PNC levels were more commonly associated with firefighters standing along the edge of the fire boundary.

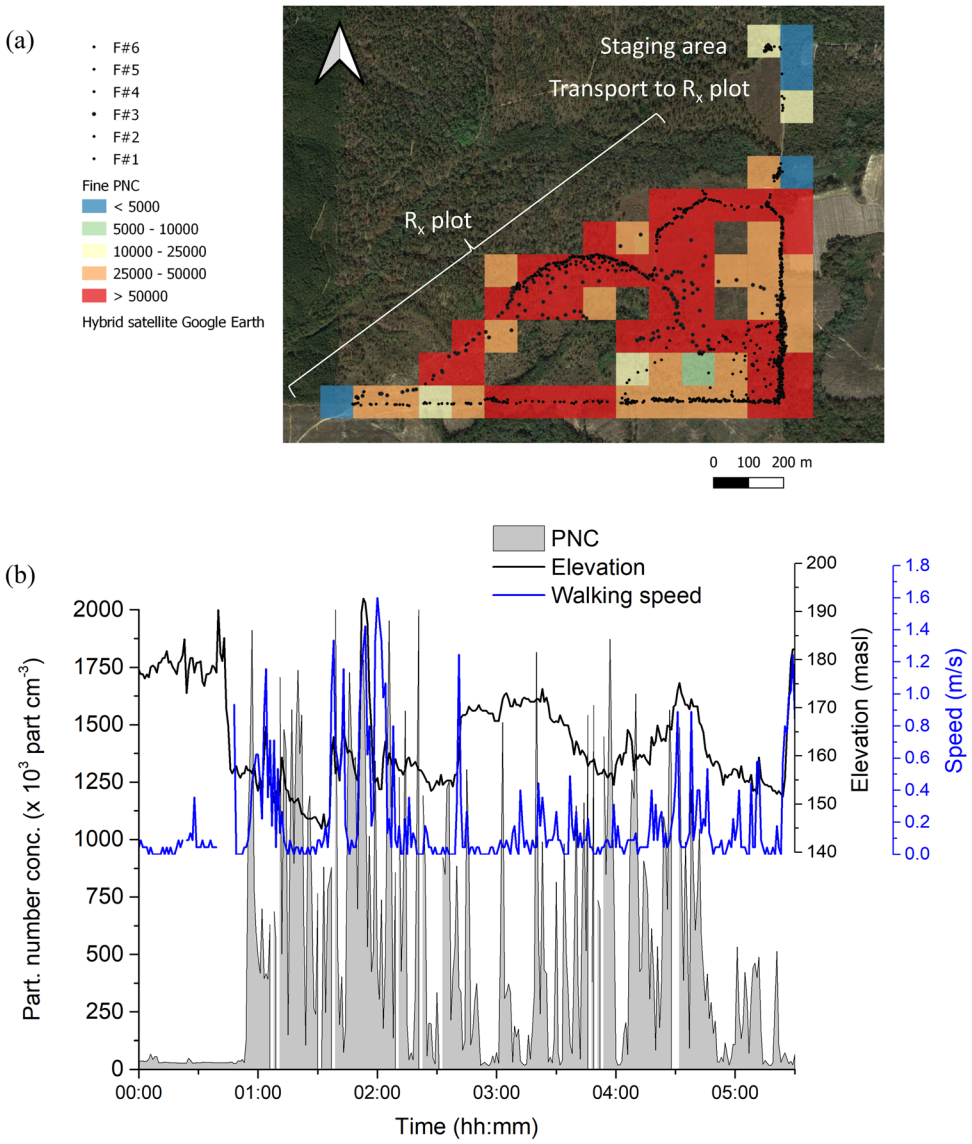

Fig. 5 **a** Gridded average PNC and the locations of firefighters in R_x #12 and **b** representative 1-min fine PNC concentration and movement (walking speed and altitude) of participant in R_x fire #12

Figure 6 shows μ and 1σ range of fine and coarse PNC and μ ± σ of walking speed for high (higher than 10,000 part L^{-1}), moderate-high (between 5,000 and 10,000 part L^{-1}) and moderate-low (between 1,200 and 5,000 part L^{-1}) fine PNC exposure periods for all R_x fires. The thresholds for moderate-low versus moderate-high were chosen to exclude measurements away from the R_x plot (or on a vehicle to/from the plot). Assuming spherical particles with a diameter of 1.8 μm and density of 1,000 kg m^{-3}, a 1-min fine PNC of 5,000 part L^{-1} corresponds to 15 μg m^{-3}. This is a conservative estimate since most of particle number is associated with ultrafine (diameter less than 100 nm) particles but their overall contribution to particle mass is limited. For both fine and coarse PNC, walking speed increased from 0.26 ± 0.03 m s^{-1} for low-moderate exposure period to 0.33 ± 0.06 m s^{-1} for moderate-high and 0.40 ± 0.03 m s^{-1} for high exposure periods (covering a distance of 15 to 24 m over a minute). While the range of measured walking speed are substantially lower than those recommended by CDC for physical activity (DHHS 2018), the association between PNC and walking speed provided an indication for the potential of higher exposures when the firefighter was in motion such as when actively maintaining the fire front through re-ignition. The increased walking pace could modify the inhaled dose because of increased breathing rate.

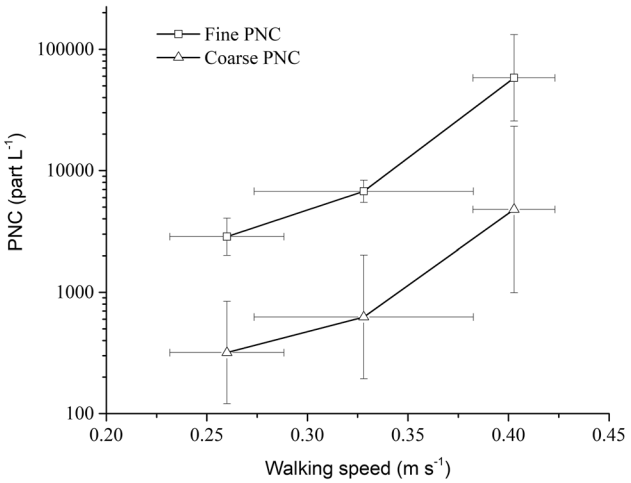

Fig. 6 Fine and coarse PNC ($\mu \pm 1\sigma$) and $\mu \pm \sigma$ walking speed of firefighters for three exposure regimes (high (> 10,000 part L^{-1}), moderate-high (between 5,000 and 10,000 part L^{-1}) and moderate-low (between 1,200 and 5,000 part L^{-1}))

Size Fractionated OC, EC and PAHs

Table 3 shows the $\mu \pm \sigma$ of OC, EC and total PAHs concentrations, abundant PAH and $\mu \pm \sigma$ of OC/EC and PAHs diagnostic ratios for the eight particle size fractions ranging from 0.52 to greater than 21.3 μm. OC concentrations varied from 2.1 ± 0.2 μg m^{-3} for particles in the 6.0–9.8 μm range to 450.7 ± 19.1 μg m^{-3} for 0.52–0.93 μm particles. Similarly, EC concentrations varied from 0.2 ± 0.1 μg m^{-3} for particles in the 6.0–9.8 μm range to 19.4 ± 2.5 μg m^{-3} for 0.93–1.55 μm particles. The OC/EC values for particles with diameter greater than 6.0 μm was lower than 4.0, while OC/EC values > 8.0 were computed for smaller particles indicating the accumulation of organic species formed during biomass burning in the accumulation mode particles. PAH concentrations varied from 7.1 ± 0.6 ng m^{-3} for particles in the 9.8–14.8 μm size range to 33.7 ± 12.2 ng m^{-3} for particles in the 0.52–0.93 μm size range. Naphthalene was the most abundant PAH for particles with diameter > 3.5 μm and pyrene was the dominant PAH for particles with diameter < 3.5 μm. Overall, PAHs were predominantly accumulated in the particle size fraction < 1.52 μm (47%; Table 3) and a MMAD of 1.90 μm. The size distribution of OC, EC and 2-,3-, 4- and 5-ring PAHs are presented in Figs. 7a–f. Low molecular weight petrogenic 2- and 3-ring PAHs were

Table 3 Personal exposures OC, EC and PAHs concentrations and concentration diagnostic ratios (**μ ± σ**) per particle size range of firefighters

	Particle size (μm)							
	> 21.3	14.8–21.3	9.8–14.8	6.0–9.8	3.5–6.0	1.55–3.5	0.93–1.55	0.52–0.93
OC (μg m^{-3})	3.7 ± 0.1	2.1 ± 0.2	3.9 ± 0.4	6.9 ± 0.7	13.2 ± 1.2	67.5 ± 3.6	167.4 ± 9.2	450.7 ± 19.1
EC (μg m^{-3})	0.8 ± 0.1	0.2 ± 0.1	0.3 ± 0.1	1.5 ± 0.2	1.6 ± 0.3	3.0 ± 1.0	19.4 ± 2.5	15.0 ± 5.1
OC/EC	4.90 ± 0.26	9.54 ± 2.78	3.07 ± 0.39	4.49 ± 0.75	8.09 ± 1.82	22.17 ± 7.15	8.64 ± 1.19	28.40 ± 9.14
Polynuclear aromatic hydrocarbons								
Abundant PAH	Nap (128)	Nap (128)	Nap (128)	Nap (128)	Nap (128)	Pyr (202)	Pyr (202)	Pyr (202)
Conc. (ng m^{-3})	11.0 ± 2.4	10.2 ± 2.3	7.1 ± 0.6	9.4 ± 1.1	7.8 ± 1.2	11.8 ± 2.9	12.4 ± 2.0	33.7 ± 12.2
Cumul. Conc	99.9	85.8	76.8	71.4	63.2	57.1	47.0	35.6
Fl/(Fl + Py)	0.50 ± 0.02	0.50 ± 0.05	0.47 ± 0.04	0.42 ± 0.03	0.47 ± 0.02	0.40 ± 0.04	0.41 ± 0.02	0.43 ± 0.01
BaA/(BaA + CT)	0.36 ± 0.03	0.39 ± 0.03	0.48 ± 0.04	0.39 ± 0.05	0.41 ± 0.06	0.52 ± 0.06	0.58 ± 0.03	0.46 ± 0.03
BeP/(BeP + BaP)	0.35	0.24 ± 0.03	0.21 ± 0.04	0.58	0.31	0.37 ± 0.16	0.36 ± 0.05	0.41 ± 0.03
IP/(IP + BgP)	0.48	0.55 ± 0.01	0.59 ± 0.08	0.51	0.55 ± 0.01	0.58 ± 0.03	0.57 ± 0.02	0.62 ± 0.03

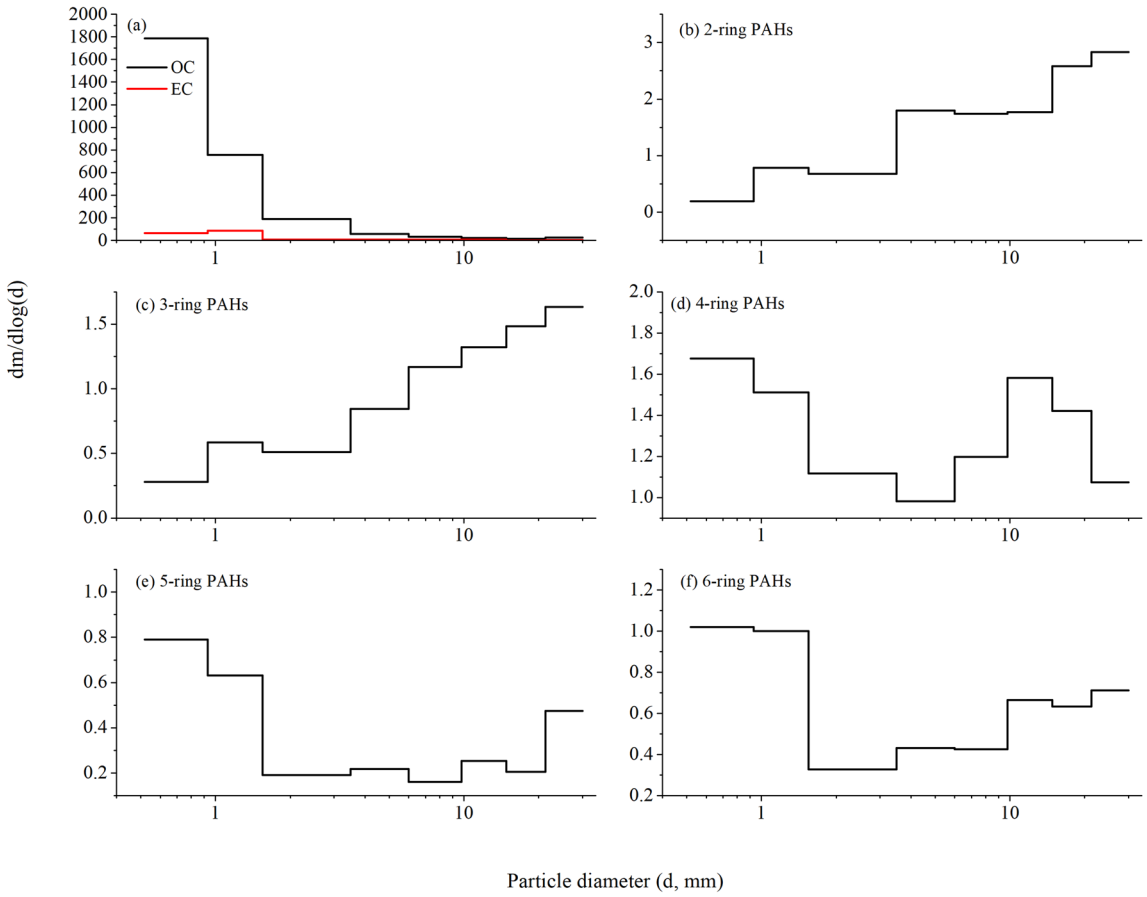

Fig. 7 Particle size concentration plots for **a** OC and EC, **b** 2-ring (naphthalene), **c** 3-ring (acenaphthene, acenaphthylene, fluorene and phenanthrene), **d** 4-ring (fluoranthene, pyrene, benz[*a*]anthacene and chrysene), **e** 5-ring (benzo[*b*]fluoranthene, benzo[*k*]fluoranthene, benzo[*e*]pyrene and benzo[*a*]pyrene) and **f** 6-ring (indeno[1,2,3-*cd*] pyrene, dibenz[*a,h*]anthracene and benzo[*ghi*]perylene)

abundant in the coarse particles size ranges ($d > 3.5$ µm) with MMAD values of 12.5 µm for naphthalene, 4.64 µm for acenaphthylene, 6.06 µm for acenaphthene, 9.07 µm for fluorene and 4.70 µm phenanthrene. On the contrary, heavier combustion 4- and 5-ring PAHs were mostly present in the fine and ultrafine size ranges and MMADs ranging from 0.18 µm for chrysene and 0.22 µm for benz(a)anthracene to 0.83 µm for benzo[a]pyrene and 1.04 µm for benzo(k) fluoranthene. The differences in the relative abundance of PAHs for different particle size ranges is related to the formation mechanisms with petrogenic PAHs being formed during the low-temperature smoldering phase and combustion PAHs during the flaming phase. *The abundance of 2- and 3-ring PAHs on coarse particle may be associated by scavenging by soil organic matter particles released at the fire front, as previously indicated by the modified OC-to-OM conversion factor and the elevated coarse particle number concentration* (Venkataraman et al. 1999). These PAHs have also been measured on the hoods of firefighters in post-municipal fire as well as in residential dust and surface water contaminated with wildfire ash suggesting that PAHs from these wildfire event have the potential to effect larger populations in addition to active duty wildland firefighters (Fent et al, 2014, Kohl et al. 2019, Manshilha et al. 2018).

A mixture of biomass and fossil fuel combustion sources were identified using PAHs concentration diagnostic ratios. This could be associated with the use of fuel (gasoline:diesel = 50:50) to start and control the fire front by crew members, in the proximity of the personal sampling. The mean [Fl/Fl + Py] ratio ranged from 0.40 ± 0.04 to 0.50 ± 0.02 that is comparable to those reported for gasoline combustion (Table 3) (Rogge et al. 1993). The ratio BaA/(BaA + CT) ratio values (from 0.36 ± 0.03 to 0.58 ± 0.03; Table 3) indicated gasoline combustion for coarse particles and biomass burning for fine particles. The mean [BeP/BeP + BaP] measured for particles in the 0.52–0.93 µm was 0.41 ± 0.03 (Table 3) similar to that reported for biomass burning; however, ratio values for larger particles indicated gasoline combustion (Rogge et al. 1993; Kavouras et al. 2012). The [IP/IP + BgP] ratios obtained in our study were

higher than 0.48 which is similar to that for fossil fuel combustion (Rogge et al. 1993).

Conclusions

Exposures to smoke aerosol of wildland firefighters were assessed over multiple prescribed fire events to facilitate monitoring under real conditions without interfering with their assigned tasks and safety. Both continuous and integrated devices were used to measure particle mass and number concentrations, OC, EC, non-exchangeable functional hydrogen types and PAHs. Smoke aerosol was mostly composed on fine particles with significant quantities of coarse particles accounting for 30% of fine and coarse PNC. Personal PNC varied greatly throughout the prescribed fires and among firefighters reflecting differences in assigned tasks, activities and location with respect to the fire front. Higher PNC levels were measured in topographies favoring the accumulation of smoke (low elevation) and for higher walking speeds as the firefighter moved within and/or along the perimeter of the burn plot. OC originated mostly from biomass burning and to a lesser extent from resuspended soil organic matter. Tracers of biomass burning (i.e. levoglucosan) and soil organic matter (i.e. formate) were detected by ^{1}H-NMR spectroscopy. The water-soluble fraction of OC consisted of a mixture of saturated oxygenated, alkyl, aryl and carboxyl groups that was consistent with the formation of phenols, polyols and polyaromatics during biomass burning. OC, EC and combustion PAHs were associated with fine particles (diameter less than 1.55 µm) with pyrene being the dominant PAHs. The abundance of heavier PAHs including benzo[a]pyrene increased as particle size decreased. The values of PAHs concentration diagnostic ratios indicated the presence of fossil fuels that may be associated with gasoline/diesel combustion to ignite and maintain the fire front as well as emissions from support vehicles. Given the scale and close proximity of wildfires to populated centers, the findings of this study may be suggestive of non-occupational exposures to wildfire smoke, too.

References

Adetona O, Simpson CD, Onstad G, Naeher LP (2013a) Exposure of wildland firefighters to carbon monoxide, fine particles, and levoglucosan. Ann Occup Hyg 57(8):979–991. https://doi.org/10.1093/annhyg/met024

Adetona O, Zhang J, Hall DB, Wang JS, Vena JE, Naeher LP (2013b) Occupational exposure to woodsmoke and oxidative stress in wildland firefighters. Sci Tot Environ 449:269–275. https://doi.org/10.1016/j.scitotenv.2013.01.075

Adler G, Flores JM, Abo Riziq A, Borrmann S, Rudich Y (2011) Chemical, physical, and optical evolution of biomass burning aerosols: a case study. Atmos Chem Phys 11:1491–1503. https://doi.org/10.5194/acp-11-1491-2011

Austin CC, Dussault G, Ecobichon DJ (2001) Municipal firefighter exposure groups, time spent at fires and use of self-contained-breathing-apparatus. Am J Ind Med 40(6):683–692. https://doi.org/10.1002/ajim.10023

Banes CJ (2014) Firefighters' cardiovascular risk behaviors: Effective interventions and cultural congruence. Workplace Health Saf 62(1):27–34

Brown DR, Alderman N, Weinberger B (2014) Outdoor wood furnaces create significant indoor particulate pollution in neighboring homes. Inhalation Toxicol 26:628–635. https://doi.org/10.3109/08958378.2014.946633

Chalbot MC, Nikolich G, Etyemezian V, Dubois DW, King J, Shafer D, Gamboa da Costa G, Hinton JF, Kavouras IG (2013) Soil humic-like organic compounds in prescribed fire emissions using nuclear magnetic resonance spectroscopy. Environ Poll 181:167–171. https://doi.org/10.1016/j.envpol.2013.06.008

Chalbot MC, Brown J, Chitranshi P, da Costa GG, Pollock ED, Kavouras IG (2014) Functional characterization of the water-soluble organic carbon of size fractionated aerosol in southern Mississippi Valley. Atmos Chem Phys 14:6075–6088. https://doi.org/10.5194/acp-14-6075-2014

Chalbot M-CG, Chitranshi P, Gamboa da Costa G, Kavouras IG (2016) Characterization of water-soluble organic matter in urban aerosol by ^{1}H-NMR spectroscopy. Atmos Environ 128:235–245. https://doi.org/10.1016/j.atmosenv.2015.12.067

Chalbot M-CG, Kavouras IG (2014) Nuclear magnetic resonance spectroscopy for determining the functional content of organic aerosols: a review. Environ Poll 191:232–249. https://doi.org/10.1016/j.envpol.2014.04.034

Chalbot M-CG, Kavouras IG (2019) NMR characterization of the water-soluble organic carbon in atmospheric aerosol. Nat Prod Comm 14(5):1–10. https://doi.org/10.1177/1934578X19849972

Chow JC, Watson JG, Crow D, Lowenthal DH, Merrifield T (2001) Comparison of IMPROVE and NIOSH carbon measurements. Aer Sci Technol 34(1):23–34. https://doi.org/10.1080/02786820119073

Daniels RD, Bertke S, Dahm MM, Yiin JH, Kubale TL, Hales TR, Baris D, Zahm SH, Beaumont JJ, Waters KM, Pinkerton LE (2015) Exposure–response relationships for select cancer and non-cancer health outcomes in a cohort of US firefighters from San Francisco, Chicago and Philadelphia (1950–2009). Occup Environ Med 2(10):699–706. https://doi.org/10.1136/oemed-2014-102671

Daniels RD, Kubale TL, Yiin JH, Dahm MM, Hales TR, Baris D, Zahm SH, Beaumont JJ, Waters KM, Pinkerton LE (2014) Mortality and cancer incidence in a pooled cohort of US firefighters from San Francisco, Chicago and Philadelphia (1950–2009). Occup Environ Med 71:388–397. https://doi.org/10.1136/oemed-2013-101662

Delfino RJ, Brummel S, Wu J et al (2008) The relationship of respiratory and cardiovascular hospital admissions to the southeastern California wildfires of 2003. Occup Environ Med 66:189–197

Duarte RMBO, Santos EBH, Pio CA, Duarte AC (2007) Comparison of structural features of water-soluble organic matter from atmospheric aerosols with those of aquatic humic substances. Atmos Environ 41:8100–8113. https://doi.org/10.1016/j.atmosenv.2007.06.034

Evarts B, Stein G (2019) U.S. Fire Department Profile. National Fire Protection Agency, Quincy, MA (https://www.nfpa.org/News-and-Research/Data-research-and-tools/Emergency-Responders/US-fire-department-profile. Accessed Feb 10, 2020)

Fabian TZ, Borgerson JL, Gandhi PD, Baxter CS, Ross CS, Lockey JE, Dalton JM (2011) Characterization of firefighter smoke exposure. Fire Technol 50:993–1019. https://doi.org/10.1007/s10694-011-0212-2

Fent KW, Eisenberg JS, Sammons D, Pleil DJ, Stiegel M, Mueller C, Horn G, Dalton J (2014) Systemic exposure to PAHs and benzene in firefighters suppressing controlled structure. Fires Ann Occup Hyg 58:830–845. https://doi.org/10.1093/annhyg/meu036

Fuzzi S, Decesari S, Facchini MC, Matta E, Mircea M, Tagliavini E (2001) A simplified model of the water soluble organic component of atmospheric aerosols. Geophys Res Lett 28:4079–4082. https://doi.org/10.1029/2001GL013418

Gaughan DM, Siegel PD, Hughes MD, Chang CY, Law BF, Campbell CR, Richards JC, Kales SF, Chertok M, Kobzik L, Nguyen PS, O'Donnell CR, Kiefer M, Wagner GR, Christiani DC (2014) Arterial stiffness, oxidative stress, and smoke exposure in wildland firefighters. Am J Ind Med 57(7):748–756. https://doi.org/10.1002/ajim.22331

Gogou A, Apostolaki M, Stephanou EG (1998) Determination of organic molecular markers in marine aerosols and sediments: one-step flash chromatography compound class fractionation and capillary gas chromatographic analysis. J Chrom 799:215–231. https://doi.org/10.1016/S0021-9673(97)01106-0

Greven F, Krop E, Spithoven J, Rooyackers J, Kerstjens H, Heederik D (2011) Lung function, bronchial hyperresponsiveness, and atopy among firefighters. Scand J Work Environ Health 37(4):325–331. https://doi.org/10.5271/sjweh.3153

Haynes HJG, Stein GP (2017) US Fire Department Profile-2015. National Fire Protection Association, Quincy, MA

Hejl AM, Adetona O, Diaz-Sanchez D, Carter JD, Commodore AA, Rathbun SL, Naeher LP (2013) Inflammatory effects of woodsmoke exposure among wildland firefighters working at prescribed burns at the savannah river site. SC J Occup Environ Hyg 10(4):173–180. https://doi.org/10.1080/15459624.2012.760064

Kavouras IG, Koutrakis P, Lagoudaki E, Tsapakis E, Stephanou EG, Oyola P, von Baer D (2001) Source apportionment of urban particulate aliphatic and polynuclear aromatic hydrocarbons (PAHs) using multivariate methods. Environ Sci Technol 35:2288–2294. https://doi.org/10.1021/es001540z

Kavouras IG, Nikolich G, Etyemezian V, DuBois D, King J, Shafer D (2012) In-situ observations of soil minerals and organic matter in the early phases of prescribed fires. J Geophys Res Atmos 117:D12313. https://doi.org/10.1029/2011JD017420

Kavouras IG, Stephanou EG (2002a) Gas/particle partitioning and size distribution of primary and secondary carbonaceous aerosol in public buildings. Indoor Air 12:17–32. https://doi.org/10.1034/j.1600-0668.2002.120104.x

Kavouras IG, Stephanou EG (2002b) Particle size distribution of organic primary and secondary aerosol constituents in urban, background marine, and forest atmosphere. J Geophys Res Atmos 107(7–8):7–17. https://doi.org/10.1029/2000JD000278

Kavouras IG, Stratigakis N, Stephanou EG (1998) Iso and anteiso-alkanes: specific tracers of environmental tobacco smoke in indoor and outdoor particle-size distributed urban aerosols. Environ Sci Technol 10:1369–1377. https://doi.org/10.1021/es970634e

Kohl L, Meng M, de Vera J, Bergquist B, Cooke CA, Hustins S, Jackson B, Chow CW, Chan AWH (2019) Limited retention of wildfire-derived PAHs and trace elements in indoor environments. Geophys Res Lett 46:383–391

Manshiha C, Duarte CG, Melo A, Ribeiro J, Flores D, Marques JE (2019) Impact of wildfire on water quality in Caramulo Mountain ridge (Central Portugal). Sustain Water Resour Manage 5:319–331. https://doi.org/10.1007/s40899-017-0171-y

Morgan G, Sheppeard V, Khalaj B et al (2010) Effects of bushfire smoke on daily mortality and hospital admissions in Sydney Australia. Epidemiology 21:47–55

Miranda A, Martins V, Casao P, Amorim JH, Valente J, Tavares R, Borrego C, Tchepel O, Ferreira AJ, Cordeiro CR, Viegas DX, Ribeiro LM, Pita LP (2010) Monitoring of firefighters exposure to smoke during fire experiments in Portugal. Environ Int 36:736–745. https://doi.org/10.1016/j.envint.2010.05.009

National Interagency Fire Center (NIFC) (2018) Fire Information-Statistics. (https://www.nifc.gov/fireInfo/fireInfo_statistics.html. Accessed Feb 2, 2020)

Northcross AL, Edwards RJ, Johnson MA, Wang ZM, Zhu K, Allen T, Smith KR (2013) A low-cost particle counter as a realtime fine-particle mass monitor. Environ Sci-Proc Imp 15:433–439. https://doi.org/10.1039/c2em30568b

Lianou M, Chalbot M-C, Kotronarou A, Kavouras IG, Karakatsani A, Katsouyanni K, Puustinnen A, Hameri K, Vallius M, Pekkanen J, Meddings C, Harrison RM, Thomas S, Ayres JG, ten Brink H, Kos G, Meliefste K, de Hartog J, Hoek G (2007) Dependence of outdoor particulate mass and number concentrations on residential and traffic features in urban areas. J Air Waste Manag Assoc 57(12):1507–1517. https://doi.org/10.3155/1047-3289.57.12.1507

Pöschl U (2005) Atmospheric aerosols: Composition, transformation, climate and health effects. Angew Chem Int Ed Engl 44(46):7520–7540. https://doi.org/10.1002/anie.200501122

Rappold AG, Stone SL, Cascio WE et al (2011) Peat bog wildfire smoke exposure in rural North Carolina is associated with cardiopulmonary emergency department visits assessed through syndromic surveillance. Environ Health Perspect 119:1415–1420

Reinhardt TE, Ottmar RD (2004) Baseline measurements of smoke exposure among wildland firefighters. J Occup Environ Hyg 1(9):593–606. https://doi.org/10.1080/15459620490490101

Rogge WF, Hildemann L, Mazurek MA, Cass GR, Simoneit BRT (1993) Sources of fine organic aerosol: 2. Noncatalyst and catalyst equipped automobiles and heavy duty diesel trucks. Environ Sci Technol 27:636–651

Schweizer D, Cisneros R, Buhler M (2019) Coarse and fine particulate matter components of wildland fire smoke at devils Postpile National Monument, California, USA. Aerosol and Air Quality Research 19:1463–1470. https://doi.org/10.4209/aaqr.2019.04.0219

Simoneit BRT, Elias VO, Kobayashi M, Kawamura K, Rushdi AI, Medeiros PM, Rogge WF, Didyk BM (2004) Sugars-dominant water-soluble organic compounds in soils and characterization as tracers in atmospheric particulate matter. Environ Sci Technol 38(22):5939–5949. https://doi.org/10.1021/es0403099

Soteriades ES, Smith DL, Tsismenakis AJ, Baur DM, Kales SN (2011) Cardiovascular disease in US firefighters: a systematic review. Cardiol Rev 19(4):202–215. https://doi.org/10.1097/CRD.0b013e318215c105

Sousan S, Koehler K, Thomas G, Park H, Hillman M, Halterman A, Peters TM (2016) Inter-comparison of low-cost sensors for measuring the mass concentration of occupational aerosols. Aer Sci Technol 50(5):462–473. https://doi.org/10.1080/02786826.2016.1162901

Steile S, Reis S, Sabel CF, Semple S, Twigg MM, Braban CF, Leeson SR, Heal MR, Harrison D, Lin C, Wu H (2015) Personal exposure monitoring of PM2.5 in indoor and outdoor microenvironments. Sci Tot Environ 508:383–394. https://doi.org/10.1016/j.scitotenv.2014.12.003

Decesari S, Fuzzi S, Facchini MC, Mircea M, Emblico L, Cavalli F, Maenhaut W, Chi X, Schkolnik G, Falkovich A, Rudich Y, Claeys M, Pashynska V, Vas G, Kourtchev I, Vermeylen R, Hoffer A, Andreae MO, Tagliavini E, Moretti F, Artaxo P (2006) Characterization of the organic com-position of aerosols from Rondônia, Brazil, during the LBA-SMOCC 2002 experiment and its representation through modelcompounds. Atmos Chem Phys 6:375–402. https://doi.org/10.5194/acp-6-375-2006

U.S. Department of Health and Human Services (DHHS) (2018) Physical activity guidelines for Americans, 2nd edn. U.S. Department of Health and Human Services, Washington, DC

Pani SK, Chantara S, Khamkaew C, Lee C-T, Lin N-H (2019) Biomass burning in the northern peninsular Southeast Asia: aerosol chemical profile and potential exposure. Atmos Res 224:180–195. https://doi.org/10.1016/j.atmosres.2019.03.031

Venkataraman C, Thomas S, Kulkarni P (1999) Size distributions of polycyclic aromatic hydrocarbons—Gas/particle partitioning to urban aerosol. J Aer Sci 30(6):759–770. https://doi.org/10.1016/S0021-8502(98)00761-7